Nuclear signaling by the APP intracellular domain occurs predominantly through the amyloidogenic processing pathway

Zoë V. Goodger[1], Lawrence Rajendran[2,3], Annette Trutzel[1], Bernhard M. Kohli[1], Roger M. Nitsch[1] and Uwe Konietzko[1]

[1]Psychiatry Research and [2]Systems and Cell Biology of Neurodegeneration, University of Zurich, August-Forel Strasse 1, 8008 Zurich, Switzerland
[3]Max-Planck Institute of Molecular Cell Biology and Genetics, Pfotenhauerstrasse 108, 01307 Dresden, Germany
*Author for correspondence (uwekon@bli.uzh.ch)

Accepted 22 July 2009
Journal of Cell Science 122, 3703-3714 Published by The Company of Biologists 2009
doi:10.1242/jcs.048090

Summary

Proteolytic processing of the amyloid precursor protein (APP) occurs via two alternative pathways, localized to different subcellular compartments, which result in functionally distinct outcomes. Cleavage by a β-γ sequence generates the Aβ peptide that plays a central role in Alzheimer's disease. In the case of α-γ cleavage, a secreted neurotrophic molecule is generated and the Aβ peptide cleaved and destroyed. In both cases, a cytosolic APP intracellular domain (AICD) is generated. We have previously shown that coexpression of APP with the APP-binding protein Fe65 and the histone acetyltransferase Tip60 results in the formation of nuclear complexes (termed AFT complexes), which localize to transcription sites. We now show that blocking endocytosis or the pharmacological or genetic inhibition of the endosomal β-cleavage pathway reduces translocation of AICD to these nuclear AFT complexes. AICD signaling further depends on active transport along microtubules and can be modulated by interference with both anterograde and retrograde transport systems. Nuclear signaling by endogenous AICD in primary neurons could similarly be blocked by inhibiting β-cleavage but not by α-cleavage inhibition. This suggests that amyloidogenic cleavage, despite representing the minor cleavage pathway of APP, is predominantly responsible for AICD-mediated nuclear signaling.

Supplementary material available online at
http://jcs.biologists.org/cgi/content/full/122/20/3703/DC1

Key words: AICD, Amyloid precursor protein, Endocytosis, Nuclear signaling, Retrograde transport

Introduction

Regulated intramembrane proteolysis (RIP) by the γ-secretase complex cleaves type I transmembrane proteins to release the intracellular domain that can subsequently translocate to the nucleus to regulate transcription (Fortini, 2002). As a prerequisite to γ-secretase-mediated cleavage, the large extracellular domain is proteolytically shed into the extracellular space. In the case of the amyloid precursor protein (APP), two alternative cleavage pathways exist, each generating different biological effects. In the amyloidogenic pathway, sequential cleavages are performed by the β-secretase BACE1 and the γ-secretase complex, generating the Aβ peptide that oligomerizes, inhibits synaptic activity, has neurotoxic properties, and aggregates into β-amyloid plaques (Hardy and Selkoe, 2002; Walsh et al., 2002). The Aβ peptide plays a central role in the pathology of Alzheimer's disease (AD), as has been formulated in the amyloid cascade hypothesis (Hardy and Higgins, 1992). Besides β-secretase cleavage, ectodomain shedding of APP can also be executed by α-secretases, including ADAM10 and TACE. This cleavage occurs inside the Aβ domain, thereby precluding the generation of toxic Aβ peptides. In addition, α-cleavage generates a soluble extracellular fragment (sAPPα) that has neurotrophic and neuroprotective activities (Mattson et al., 1993). These opposing biological outcomes of RIP processing for APP are so far unique amongst the described RIP substrates.

The subcellular localization and trafficking of APP strongly influences its mode of processing. Aβ secretion is greatly reduced in Chinese Hamster Ovary (CHO) cells expressing APP with a deletion of the YENPTY sequence necessary for endocytosis (Koo and Squazzo, 1994; Perez et al., 1999). The endocytosis of APP has been shown to occur after its accumulation with BACE1 in lipid rafts, and the production of Aβ is cholesterol-dependent (Ehehalt et al., 2003). Expression of dominant-negative dynamin to block endocytosis reduced Aβ and simultaneously increased APP levels at the plasma membrane and increased sAPPα secretion (Carey et al., 2005; Ehehalt et al., 2003). By contrast, the enhancement of endocytosis by overexpression of Rab5 favors Aβ production (Grbovic et al., 2003). A recent report has demonstrated that sAPPβ, the extracellular domain generated by β-secretase cleavage, resides in endosomes. This suggests that β-cleavage occurs after endocytosis of APP from the cell surface (Rajendran et al., 2006), in line with the reported endosomal localization and acidic pH optimum of BACE1 activity (Huse et al., 2000; Lin et al., 2000; Vassar et al., 1999). Analysis of APP-BACE1 interactions by fluorescence resonance energy transfer (FRET) has further confirmed that the strongest association between APP and BACE1 occurs within endosomes (Kinoshita et al., 2003). Finally, analysis of late endosomes by microscopy detected the presence of APP, suggesting that a fraction of endocytosed APP is not recycled to the plasma membrane (Ferreira et al., 1993; Rajendran et al., 2006).

In contrast to endosomal β-cleavage of APP, the production of sAPPα occurs at the plasma membrane (Sisodia, 1992) and is enhanced when endocytosis is inhibited and APP accumulates at the plasma membrane (Carey et al., 2005; Ehehalt et al., 2003; Neumann et al., 2006).

Following ectodomain shedding by α- or β-secretase, the membrane-bound α- and β-stubs are multiply cleaved by the γ-secretase complex, whereby the primary ε-cleavage releases the APP intracellular domain (AICD) (Fukumori et al., 2006; Kakuda et al., 2006). Because γ-secretase is present at the plasma membrane (Chyung et al., 2005; Tarassishin et al., 2004), in addition to intracellular compartments such as endoplasmic reticulum (ER) and Golgi (Annaert et al., 1999), AICD can also be generated at the plasma membrane, spatially distinct from AICD generated after β-γ cleavage in the endosomal system.

AICD has a short half-life and is rapidly degraded (Cupers et al., 2001), for instance by insulin-degrading enzyme (Edbauer et al., 2002). We therefore hypothesized that AICD generated by sequential α-γ or β-γ-cleavages would have different propensities for translocating to the nucleus. The APP-binding protein Fe65 stabilizes AICD (Kimberly et al., 2001) and stimulates the transactivating activity of AICD in Gal4-promoter luciferase assays (Cao and Sudhof, 2001). We have previously shown that AICD is transported to the nucleus by Fe65 where together they bind Tip60, localize into spherical nuclear complexes (termed AFT complexes), and regulate transcription (Konietzko et al., 2008; von Rotz et al., 2004).

To determine the contribution of α- and β-secretase-mediated processing of APP to nuclear signaling by AICD, we analyzed the formation of nuclear AFT complexes while biasing APP processing towards either α- or β-cleavage pathways using genetic and pharmacological approaches. Furthermore, we blocked endocytosis to enhance α-cleavage and prevent β-secretase processing, and manipulated both active retrograde and anterograde transport systems. Finally, we analyzed the effect of secretase inhibition on the nuclear translocation of endogenous AICD in primary neurons. Together, our results point towards the endosome-based β-secretase-mediated processing pathway of APP in generating AICD capable of nuclear signaling.

Results

We have previously shown that AICD cleaved from APP translocates to the nucleus bound to Fe65, forms spherical nuclear AFT complexes together with Tip60, and is transcriptionally active (Konietzko et al., 2008; von Rotz et al., 2004). Here, we determined the nuclear signaling capability of AICD by analyzing the formation of AFT complexes, while influencing subcellular trafficking and proteolytic processing of APP through both genetic and pharmacological manipulations.

Inhibition of endocytosis blocks nuclear translocation of AICD

Dynamin GTPase is central in the pinching-off of vesicles during endocytosis and thus plays a role in the transfer of cell-surface APP to endosomes, where BACE1 cleavage is dominant (Carey et al., 2005; Kinoshita et al., 2003). The K44A dynamin mutant, where the GTP-binding consensus sequence is altered, acts in a dominant-negative fashion to inhibit endocytosis when overexpressed (Herskovits et al., 1993). The dominant-negative dynamin indeed inhibited endocytosis of holotransferrin, as shown by the reduced uptake in the Dyn K44A-expressing cells (supplementary material Fig. S1). HEK293 cells were transfected with APP, tagged with Citrine at the C-terminus, and with N-terminally Myc-tagged Fe65 and CFP-Tip60, which led to nuclear AFT complex formation. To manipulate endocytosis, we additionally transfected either wild-type or K44A mutant dynamin, both fused to a hemagglutinin (HA) tag to enable detection. Analysis by confocal microscopy revealed that cells expressing wild-type dynamin were capable of forming AFT complexes (Fig. 1A). Compared to wild-type dynamin, the number of nuclei with AFT complexes was strongly reduced when K44A dynamin was co-transfected (Fig. 1B). The block of nuclear AICD translocation only occurred at higher expression levels of the dominant-negative mutant (Fig. 1B, lower panel). Therefore, in cells transfected with all four constructs, the expression of K44A mutant dynamin might not always attain levels sufficient to compete with endogenous dynamin and block endocytosis. Quantification of the number of cells with AFT complexes nevertheless revealed a significant reduction in AFT complexes in cells expressing K44A mutant dynamin compared to the wild-type construct (Fig. 1C) [n=4, Mann-Whitney U test (MWU) P<0.05].

Inhibition of endocytosis reduces β-cleavage of APP

To investigate the effects of inhibiting endocytosis on the β-cleavage of APP, we utilized a cell line with stable expression of APP that was labeled at its C-terminus with a triple HA tag, and analyzed protein levels of the β-cleaved C-terminal fragment of APP (β-CTF). Cells were transfected with wild-type or K44A mutant dynamin, or with mRFP as a transfection control, and treated with the γ-secretase inhibitor DAPT for 22 hours to accumulate APP CTFs. Western blot analysis revealed a significant reduction in the amount of β-CTF after inhibition of endocytosis through expression of K44A dynamin, whereas levels of full-length APP remained unchanged (Fig. 2A,B) (n=3, MWU, P<0.05). In addition, we transfected HeLa cells with Swedish mutant APP (SwAPP) fused to CFP, together with either GFP-tagged dominant-negative dynamin, or GFP as a control. Using an antibody that specifically detects sAPPβ generated from SwAPP (Rajendran et al., 2006), we saw prominent labeling of endosomes in control transfected cells (Fig. 2C). When endocytosis was inhibited in cells transfected with the K44A dynamin mutant, the generation of sAPPβ was greatly reduced (Fig. 2D). Inhibiting endocytosis therefore reduces β-secretase cleavage of APP and nuclear signaling by AICD.

BACE1 inhibition reduces AFT complex formation, whereas enhancing β-cleavage increases nuclear signaling by AICD

In order to manipulate β-secretase-mediated cleavage of APP, we biased APP processing towards the non-amyloidogenic pathway using a BACE1 inhibitor. A tripeptide-based inhibitor with an IC50 of 700 nM, previously tested in cell culture (Abbenante et al., 2000), was applied in a dilution series, ranging from twofold IC50 down to DMSO vehicle only. A HEK293 cell-line constitutively expressing APP-Citrine was co-transfected with Fe65 and Tip60. With increasing concentration of BACE1 inhibitor, the formation of nuclear AFT complexes was reduced (correlation coefficient, –0.984) (Fig. 3A). This reduction was found to be significant in the twofold-IC50-treated cells compared to the vehicle-treated control (n=3, MWU P<0.05). In order to monitor whether the inhibitor concentrations used resulted in the inhibition of BACE1, we treated wild-type HEK293 cells using the same dilution series as for the fluorescence microscopy experiments. Cells were treated concomitantly with the γ-secretase inhibitor DAPT in order to accumulate levels of APP CTFs. Western blot analysis using an APP C-terminal antibody revealed a clear reduction in the β-CTF

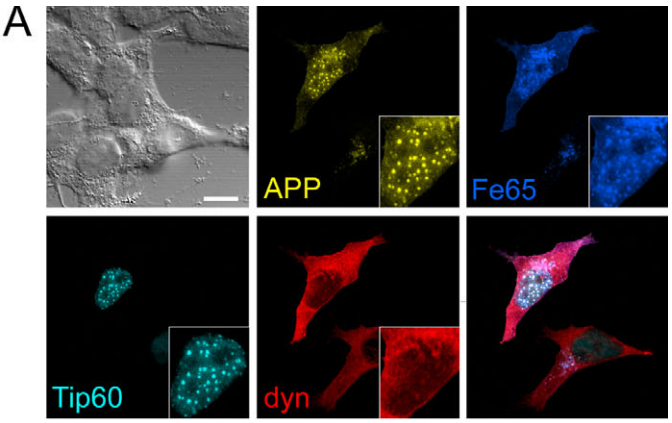

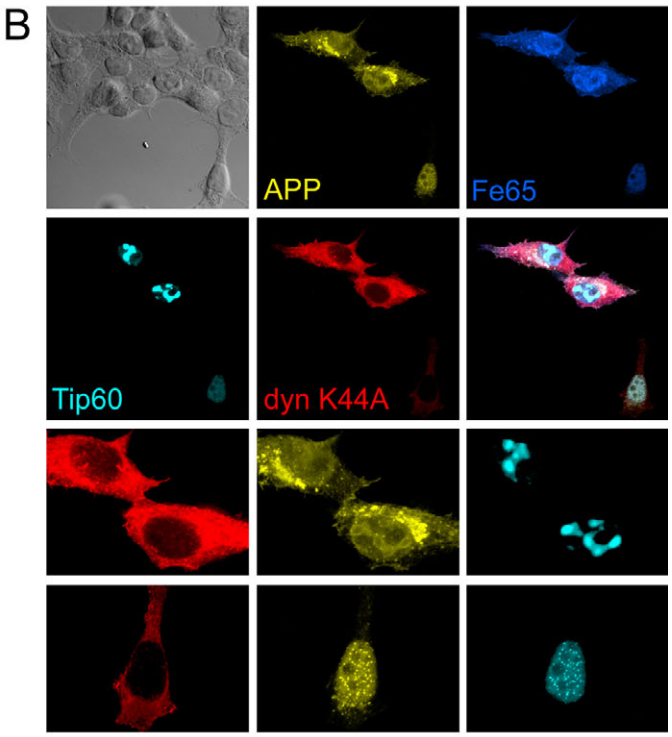

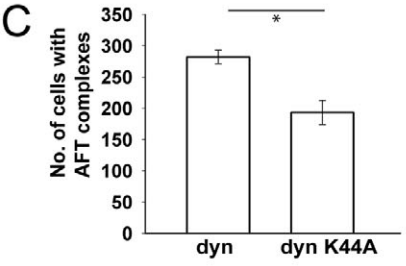

Fig. 1. Inhibition of endocytosis blocks nuclear translocation of AICD. (A) Confocal microscopy of cells transfected with APP-Citrine (APP), Myc-Fe65 (FE65) and CFP-Tip60 (Tip60), together with wild-type, HA-labeled dynamin (dyn) shows clear formation of nuclear AFT complexes. Inserts are magnified twofold. Scale bar: 13 µm. (B) Confocal microscopy of cells co-transfected with dyn K44A mutant blocks the formation of nuclear AFT complexes, despite the coexpression of APP, Fe65 and Tip60. Tip60 localizes to nuclear speckle-like structures in contrast to the spherical spots where it co-localizes with Fe65 and AICD. Imaging cells at twofold higher magnification (lower panels) shows that a high expression of dominant-negative dynamin is necessary to block nuclear signaling. AFT complexes are still observed in cells with low dyn K44A expression (bottom row). Scale is 20 µm in B upper panels (overview). (C) Quantification of AFT complex formation in cells co-transfected with APP, Fe65 and Tip60, together with either wild-type (dyn) or K44A mutant dynamin (dyn K44A). Values were normalized to the average level of Cy3 fluorescence in cells transfected with wild-type dynamin. Error bars represent s.e.m., n=4, *P<0.05, MWU.

to α-CTF ratio with increasing inhibitor concentrations, verifying that the dilution series encompassed the relevant range (Fig. 3B).

In order to show that the endocytic BACE1 cleavage is responsible for AICD signaling, we repeated these experiments using a sterol-linked membrane-anchored β-secretase inhibitor (Rajendran et al., 2008) that is targeted to early endosomes and specifically inhibits endosomally localized BACE1. HEK293 cells were transfected with APP, Fe65 and Tip60, followed by 16 hours of treatment with 1 µM sterol-linked inhibitor. Formation of AFT complexes was significantly reduced in cells treated with BACE1 inhibitor compared to DMSO-treated controls (Fig. 3C) (n=3, MWU P<0.05). To assess the effects of the sterol-linked inhibitor on APP processing, HEK293 cells with stable expression of APP-3HA were treated with or without inhibitor for 16 hours and the protein lysates analyzed by western blotting. There was a dramatic reduction in β-CTF levels after inhibitor treatment, which was seen most clearly in cells treated concomitantly with the γ-secretase inhibitor DAPT (Fig. 3D).

Because the inhibition of β-secretase has been shown to reduce AICD-mediated nuclear signaling, increasing BACE1 cleavage of APP might be expected to have the reverse effect. The Swedish mutation of APP, reported in specific cases of familial AD, has a higher affinity for BACE1 and consequently results in greater production of β-CTFs (Citron et al., 1994; Haass et al., 1995). We transfected cells with Citrine-labeled wild-type or Swedish mutant APP, in addition to Tip60 and Fe65. Quantification of the number of cells with nuclear AFT complexes revealed a significant increase in cells expressing the Swedish mutant compared to wild-type APP (Fig. 3E) (n=6, P<0.05, MWU). In addition, cells were transfected with either wild-type APP-3HA or SwAPP-3HA and lysates analyzed by western blotting. There was a clear increase in the level of β-CTF generated by cells expressing the Swedish mutant (Fig. 3F), suggesting that increasing APP cleavage by BACE1 increased AICD signaling.

Our results using pharmacological inhibition of BACE1 pointed towards a role of the β-secretase-mediated cleavage pathway in AICD-mediated nuclear signaling. In order to further determine the physiological relevance of this finding, we utilized a genetic model in which the BACE1 gene is inactivated. BACE1 knockout fibroblasts, derived from BACE1-deficient mice (Dominguez et al., 2005), were transfected with APP, Fe65 and Tip60 and their ability to form AFT complexes was compared to wild-type fibroblasts using confocal microscopy (Fig. 4A,B). Although fibroblasts show markedly reduced transfection efficiencies in comparison to HEK293 cells, we could clearly identify nuclear AFT complexes in wild-type fibroblasts. By contrast, AICD nuclear signaling was almost abolished in BACE1-deficient cells (Fig. 4C) (n=3, MWU P<0.05). Therefore, β-secretase-mediated cleavage of APP appears to be essential for AICD signaling to the nucleus and formation of AFT complexes. Furthermore, in cells deficient in the α–secretase ADAM10 we could also identify AFT complexes in the nucleus (supplementary material Fig. S2). The transfection efficiency of ADAM10 knockout fibroblasts was even lower than for wild-type and BACE1 knockout fibroblasts, preventing a quantification of cells harboring nuclear AFT complexes.

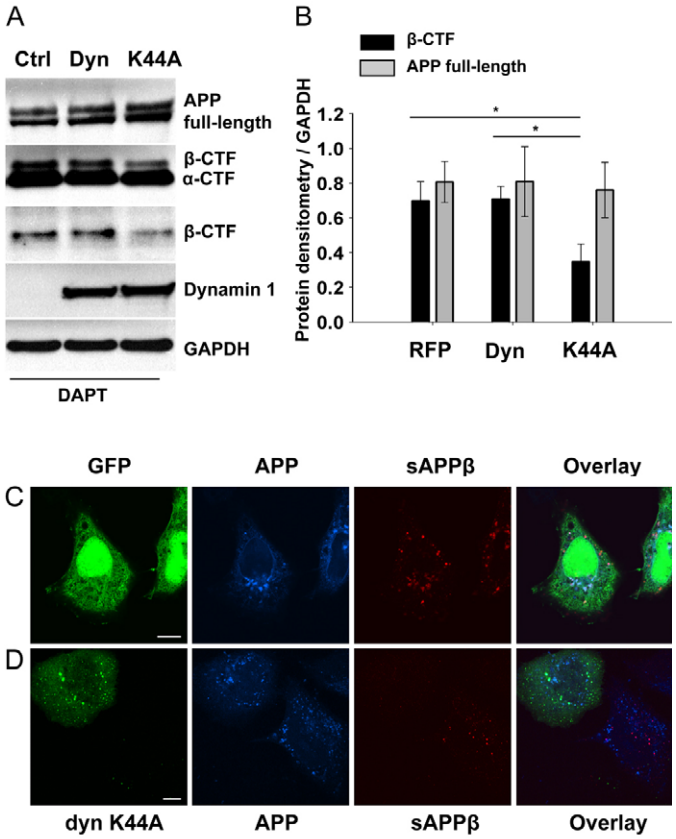

Fig. 2. Inhibition of endocytosis reduces β-cleavage of APP. (A) HEK293 cells, stably expressing C-terminally labeled APP-3HA, were transfected with wild-type (Dyn) or K44A mutant dynamin (K44A), or mRFP as transfection control (Ctrl), and treated with the γ-secretase inhibitor DAPT for 22 hours to accumulate APP CTFs. Western blotting and staining were carried out using anti-HA-tag antibody to detect levels of full-length APP and both α- and β-CTFs, and 6E10 antibody to specifically detect β-CTFs. A reduction in βCTF levels is clearly visible in cells expressing the K44A mutant. (B) Quantification of β-CTF and full-length APP after transfection of cells as described in A reveals a significant reduction in β-CTF levels after inhibition of endocytosis with K44A dynamin. Levels of full-length APP are not significantly altered. Error bars represent s.e.m., n=3, *P<0.05, MWU. (C,D) HeLa cells were co-transfected with SwAPP-CFP and either dominant-negative dyn K44A-GFP or GFP as a control. Staining with a polyclonal antibody was used to detect the ectodomain of β-cleaved SwAPP (sAPPβ). (C) GFP control-transfected cells show prominent generation of sAPPβ in endosomal compartments. (D) Expression of dyn K44A prevents the generation of sAPPβ. Scale bars: 10 μm.

Translocation of AICD to the nucleus is mediated by active retrograde transport

Because our results pointed strongly towards the endocytic β-secretase-mediated processing pathway of APP as the mediator of nuclear signaling, we analyzed the subcellular distribution of endocytosed APP by performing antibody uptake experiments. HEK293 cells were transfected with APP fused at the C-terminus to three tandem HA tags and incubated with the 6E10 antibody that binds between the β- and α-cleavage site of APP. Binding at 4°C, to prevent endocytosis, showed prominent surface-labeling of transfected cells (Fig. 5A). Following 6E10 binding, the cells were incubated for 10 or 30 minutes at 37°C. After 10 minutes, there was already 6E10 staining in vesicles close to the nucleus (Fig. 5B). At 30 minutes, the vast majority of the surface-bound 6E10 had been endocytosed and translocated to perinuclear regions, where

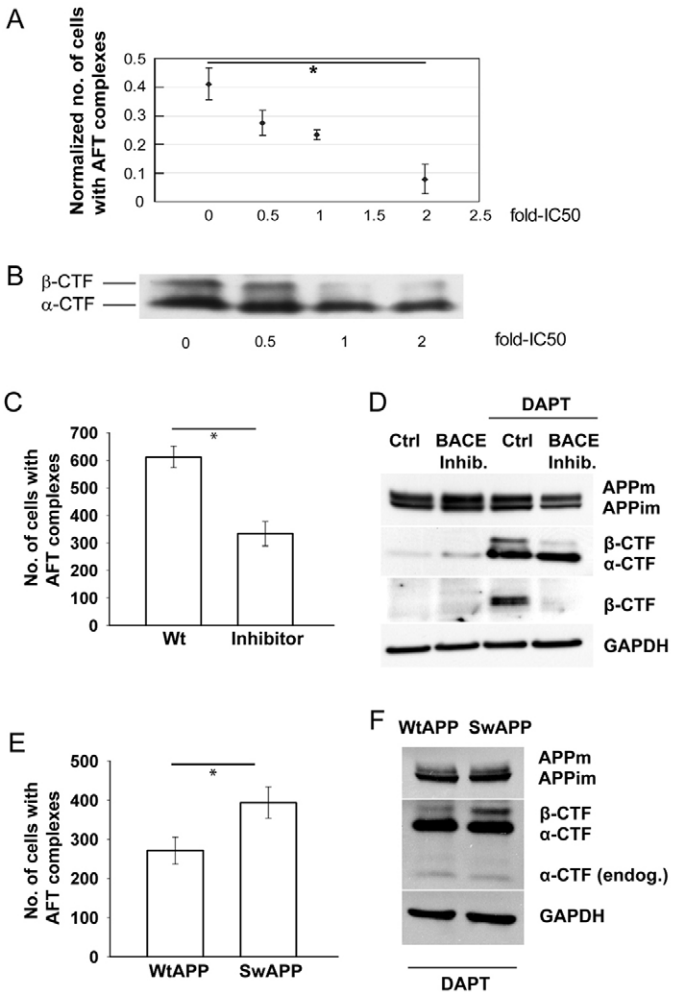

Fig. 3. BACE1 inhibition reduces AFT complex formation, whereas enhancing β-cleavage increases nuclear signaling by AICD. (A) HEK293 cells transfected with wild-type human APP-Citrine, CFP-Tip60 and Myc-Fe65 were treated for 22 hours with DMSO vehicle only or with β-secretase inhibitor at different concentrations (IC50=700 nM). Correlation between the fold-IC50 and the number of cells containing AFT complexes was clearly negative (–0.984). Inhibition relative to control was significant at twofold IC50 (n=3, *P<0.05, MWU). (B) HEK293 cells expressing endogenous APP were treated simultaneously with γ-secretase inhibitor (to accumulate CTFs) and β-secretase inhibitor at the concentrations indicated. Western blotting with an APP C-terminal antibody shows the inhibition of β-CTF formation around and above the IC50 concentration. (C) HEK293 cells were transfected with APP-Citrine, HA-Fe65 and CFP-Tip60, followed by 16 hours treatment with 1 μM sterol-linked BACE1 inhibitor. AFT complex formation was significantly reduced in cells treated with BACE1 inhibitor compared to DMSO-treated controls (Wt). n=3, *P<0.05, MWU. (D) Cells stably expressing APP-3HA were treated with or without inhibitor for 16 hours and total protein lysates analyzed by western blotting. Membranes were probed using anti-HA-tag antibody to detect levels of full-length APP and both α- and β-CTFs, and using 6E10 antibody to specifically detect β-CTFs. Levels of β-CTFs are reduced dramatically after inhibitor treatment, which is especially visible in cells treated concomitantly with 1 μM DAPT. (E) HEK293 cells transfected with either wild-type (WtAPP) or Swedish mutant (SwAPP) APP-Citrine, in addition to CFP-Tip60 and HA-Fe65. Quantification of the number of cells with nuclear AFT complexes reveals a significant increase in AFTs in cells expressing the Swedish mutant compared to wild-type APP. Error bars represent s.e.m., n=6, *P<0.05, MWU. (F) Cells were transfected with either wild-type APP-3HA or SwAPP-3HA and lysates analyzed by western blotting. Analysis using APP C-terminal antibody, which detects both endogenous and HA-labeled APP, reveals a strong increase in β-CTFs in cells expressing the SwAPP mutant. Error bars represent s.e.m. in A, C and E. APPm, mature APP; APPim, immature APP.

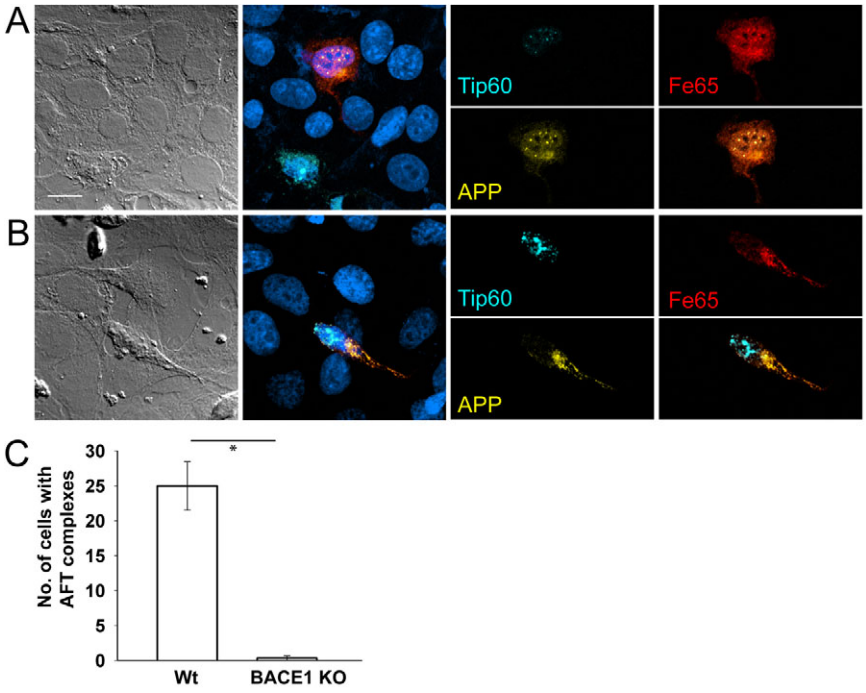

Fig. 4. BACE1 knockout fibroblasts lack AICD-mediated nuclear signaling. (A) Wild-type fibroblasts were transfected with APP-Citrine, HA-Fe65 and CFP-Tip60 and analyzed by confocal microscopy. Images show clear formation of spherical AFT complexes. (B) BACE1 knockout fibroblasts fail to show translocation of AICD-Fe65 to the nucleus, and Tip60 resides in irregular speckles when transfected as in A. Larger left images show differential interference contrast and overlay of fluorescent stainings with nuclear DRAQ5 staining. Single fluorescent channels are shown in the cutouts on the right. Scale bar: 13 µm. (C) Quantification of the number of cells with AFT complexes reveals a near-abolishment of AFT complex formation in the BACE1 knockout (BACE1 KO) fibroblasts compared to wild-type (Wt). Error bars represent s.e.m., n=3, *P<0.05, MWU.

it colocalized with APP detected via the HA tags (Fig. 5C). Therefore, either full-length APP or β-CTFs, both detected by the 6E10 and anti-HA antibodies, are transported from the plasma membrane to the vicinity of the nucleus.

To determine the involvement of active retrograde transport in the perinuclear translocation of APP and β-CTFs, we disrupted the dynein-dynactin complex. Dynactin is a multi-protein complex that is involved in coordinating binding of cargo vesicles to dynein for minus-directed transport along microtubules from the periphery to the soma. Overexpression of p50 dynamitin (Burkhardt et al., 1997) or p150^{Glued} (Quintyne et al., 1999), both subunits of dynactin, results in the uncoupling of the dynactin complex from dynein and disruption of retrograde transport. We transfected cells with APP-Citrine, HA-Fe65 and CFP-Tip60 to generate AFT complexes, and additionally with either p50 dynamitin-GFP or p150^{Glued}-mRFP (only with coiled-coil domain 1; CC1); GFP and mRFP, respectively, were used as control vectors. Analysis by confocal microscopy revealed many cells expressing all four constructs. In the case of cells overexpressing either of the dynactin components, nuclear AFT complex formation was inhibited and Tip60 was localized to

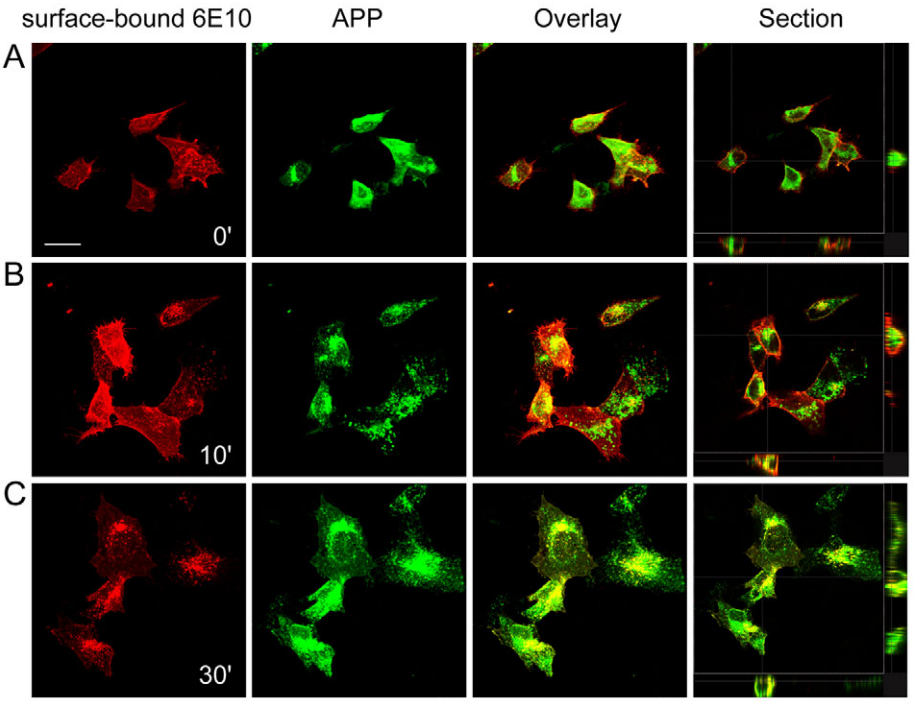

Fig. 5. APP is endocytosed from the plasma membrane and transported to perinuclear compartments. Live HEK293 cells transfected with APP-3HA were incubated for 30 minutes at 4°C to allow binding of 6E10 antibody to cell-surface APP. (A) Confocal microscopy of cells fixed immediately after the 4°C incubation. Staining for 6E10 reveals strong surface binding on cells expressing APP-3HA. (B) Incubation of cells at 37°C leads to the endocytosis of surface APP together with the bound 6E10 antibody, with vesicles seen close to the nucleus after 10 minutes. (C) After 30 minutes most of the 6E10 has been translocated to perinuclear compartments. Scale bar: 30 µm in A; 20 µm in B and C.

nuclear speckles. Additionally, APP and Fe65 were often seen to accumulate in the processes (Fig. 6A). As observed with the expression of dynamin mutants that inhibit endocytosis, a threshold level of expression is necessary to inhibit cellular processes. We determined the number of cells with AFT complexes with a fluorescence microscope and found that coexpression of p50 dynamitin-GFP significantly reduced the formation of nuclear AFT complexes when compared to coexpression of GFP as a control (Fig. 6B) (n=4, P<0.05, MWU). Similarly, the disruption of retrograde transport by p150^{Glued}-mRFP expression resulted in reduced formation of nuclear AFT complexes compared to that seen with transfection of mRFP (Fig. 6C) (n=3, P<0.05, MWU).

To analyze the effect of inhibiting retrograde transport on β-cleavage of APP, HEK293 cells with stable expression of APP-3HA were transfected with either p50 dynamitin-GFP or p150^{Glued}-mRFP. mRFP was used as a transfection control. Western blot analysis using 6E10 antibody revealed a reduction in the levels of β-CTFs in cell lysates after the disruption of the dynein-dynactin complex by the overexpression of either p50 dynamitin or p150^{Glued} (Fig. 6D). Therefore, inhibition of retrograde transport both disrupts β-cleavage of APP and inhibits nuclear signaling by AICD.

Targeting endosomes to the cell periphery blocks AICD-mediated nuclear signaling

Having identified a role of active retrograde transport in nuclear signaling by AICD, we hypothesized that modification of anterograde transport or perturbation of the subcellular organization of endosomes might also influence AICD signaling. Anterograde transport is mediated by kinesin (KIF) motors; KIF16B is a kinesin-3 motor that specifically transports endosomes to the plus end of microtubules (Hoepfner et al., 2005). The overexpression of KIF16B has been shown to relocate early endosomes to the cell periphery, whereas the expression of dominant-negative KIF16B-ΔN, which lacks the catalytic domain, causes the clustering of early endosomes to the perinuclear region and delays receptor recycling to the plasma membrane (Hoepfner et al., 2005). Expression of wild-type KIF16B, labeled with yellow fluorescent protein (YFP), showed a localization mostly in the cell periphery, whereas the YFP-labeled dominant-negative mutant localized within the perinuclear region of the cell (Fig. 7A). When coexpressed with APP, Fe65 and Tip60, overexpression of wild-type KIF16B inhibited the formation of nuclear AFT complexes, when viewed in the confocal microscope, whereas dominant-negative KIF16B clearly enabled AFT complex formation (Fig. 7B). When quantified, the number of cells with AFT complexes was found to be significantly reduced in cells treated with wild-type KIF16B, both compared to control (mRFP-transfected) and dominant-negative KIF16B-transfected cells (Fig. 7C) (n=4, MWU P=<0.05). There was, however, no significant difference between control and KIF16B dominant-negative treated cells, despite a trend towards an increase in AFT numbers. To analyze the effects of KIF16B expression on APP βCTF levels, HEK293 cells expressing APP-3HA were transfected with KIF16B constructs or with mRFP as a control and additionally treated for 22 hours with DAPT to prevent degradation of the APP CTFs produced. Western blotting using both anti-HA and 6E10 antibodies revealed an increase in βCTFs in cells treated with dominant-negative KIF16B. Further, there was both an increase in αCTFs and a reduction in βCTFs in cells treated with wild-type KIF16B (Fig. 7D). Therefore, overexpression of wild-type KIF16B leads to a reduction of β-secretase-mediated cleavage of APP,

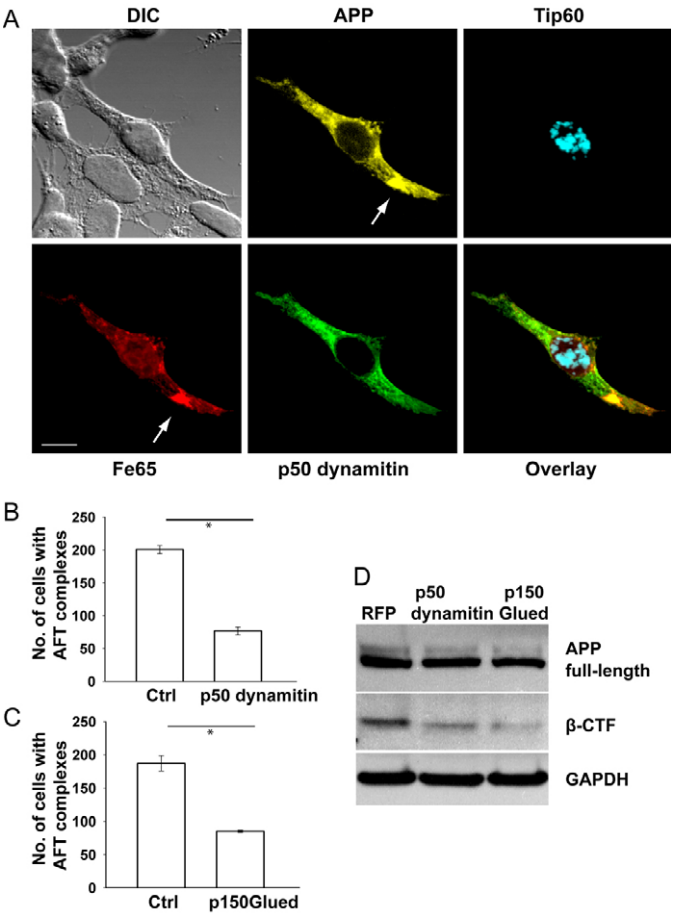

Fig. 6. Nuclear translocation of AICD depends on active retrograde transport. Overexpression of components of the dynactin complex block dynein-mediated retrograde transport. (A) Confocal microscopy of HEK293 cells co-transfected with APP-Citrine, CFP-Tip60, HA-Fe65 and p50 dynamitin-GFP. Tip60 localizes to nuclear speckle-like compartments and nuclear translocation of AICD is completely prevented. Accumulation of APP and Fe65 in the processes is frequently observed (arrows). Scale bar: 10 μm. (B) Cells were transfected with APP-Citrine, CFP-Tip60, HA-Fe65 and either p50 dynamitin-GFP or GFP as a control. Quantification of cells with AFT complexes shows a significant reduction when retrograde transport is inhibited by the expression of p50 dynamitin. Error bars represent s.e.m., n=4, *P<0.05, MWU. (C) Cells were transfected as in B to generate AFT complexes with co-transfection of either RFP-p150^{glued} CC1 domain, to inhibit retrograde transport, or RFP as a control. Quantification of cells with AFT complexes shows a significant reduction when retrograde transport is inhibited by the expression of p150^{glued} CC1. Error bars represent s.e.m., n=3, *P<0.05, MWU. (D) HEK293 cells expressing APP-3HA were transfected with either p50 dynamitin-GFP or p150^{glued} CC1-RFP. mRFP was used as a transfection control. Cells were treated for 22 hours with 1 μM DAPT and total cell lysates analyzed by western blotting. Membranes were probed using 6E10 antibody to detect levels of full-length APP and β-CTFs. Cells transfected with either p50 dynamitin or p150^{glued} show reduced levels of β-CTFs compared to mRFP-transfected cells.

whereas expression of its dominant-negative form has the reverse effect. Together, these data point to a role for perinuclear endosomes in AICD nuclear signaling.

BACE1 inhibition in primary neurons inhibits endogenous AICD nuclear signaling

Our results using both pharmacological and genetic inhibition of BACE1 in HEK293 cells and fibroblasts highlighted an important role for the β-secretase-mediated cleavage pathway of APP in AICD

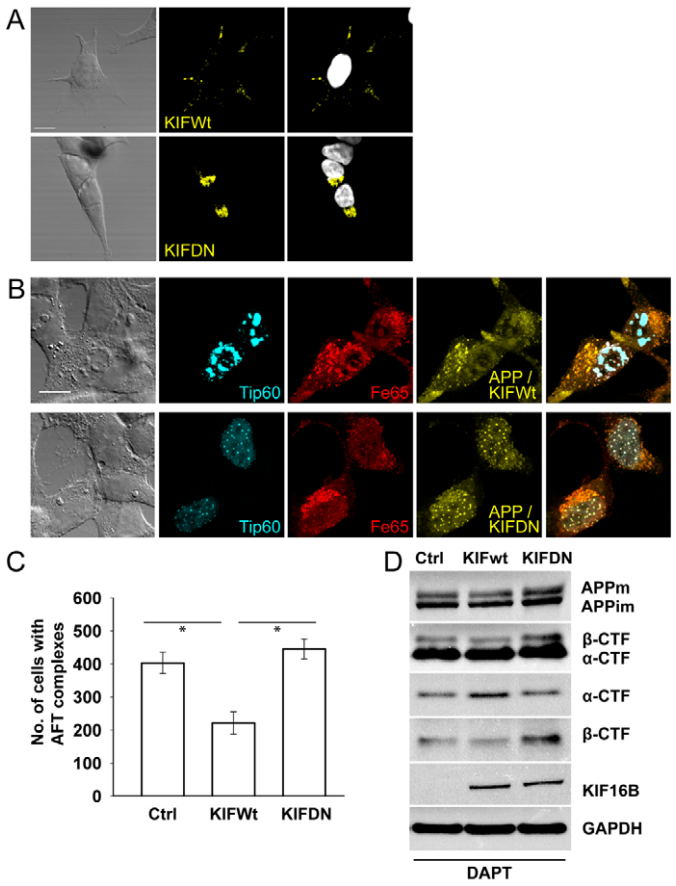

Fig. 7. Targeting endosomes to the cell periphery blocks AICD-mediated nuclear signaling. (A) KIF16B is the motor protein responsible for anterograde transport of endosomes. Overexpression of wild-type KIF16B-YFP (KIFWt) in HEK293 cells shows localization mostly in the cell periphery, whereas expression of KIF16B-ΔN-YFP (KIFDN) is predominantly localized within the perinuclear region. Left panels show differential interference contrast; middle panels the YFP fluorescence; and right panels the overlay of YFP with DAP1-labeled nuclei. Cells were counterstained with DAPI to label nuclei. (B) Confocal microscopy of HEK293 cells transfected with APP, Fe65, Tip60 and KIF16B constructs. Overexpression of wild-type KIF16B inhibits the formation of nuclear AFT complexes, whereas dominant-negative KIF16B clearly enables formation of AFT complexes. Left panels show differential interference contrast, and far right panels the overlay of the fluorescent stainings. Scale bars: 13 µm. (C) Quantification reveals the number of cells with AFT complexes to be significantly reduced in cells treated with wild-type KIF16B, both compared to control (mRFP-transfected) and dominant-negative KIF16B-transfected cells. Error bars represent s.e.m., n=4, *P<0.05, MWU. (D) Analysis of the effect of wild-type and dominant-negative KIF16B expression on APP βCTF levels. HEK293 cells expressing APP-3HA were transfected with KIF16B constructs or with mRFP as control and additionally treated for 22 hours with DAPT to accumulate APP CTFs. Western blotting and staining were carried out using anti-HA-tag antibody to detect full-length APP and both α- and β-CTFs, and using 6E10 antibody to specifically detect β-CTFs. To control for transfection efficiency, KIF16B-YFP constructs were detected using GFP antibody. Levels of β-CTF are increased in cells overexpressing dominant-negative KIF16B. In cells overexpressing wild-type KIF16B, levels of β-CTF are reduced, whereas levels of α-CTF are increased.

nuclear signaling. In order to further confirm the physiological relevance of our findings, we analyzed the occurrence of endogenous AICD in the nuclei of primary neurons. We have previously shown the formation of endogenous nuclear AICD spots to be enhanced through the inhibition of nuclear export using leptomycin B (LMB) (Konietzko et al., 2008). Primary neuronal cultures, isolated from postnatal day zero C57/Bl6 mice, were treated after 14 days in vitro (DIV 14) with 20 ng/ml LMB for 22 hours, followed by nuclei preparation and immunoprecipitation. Western blotting and staining using anti APP C-terminal antibody revealed a marked increase in the levels of AICD detected after LMB treatment compared to control conditions (Fig. 8A). To visualize endogenous AICD in the nucleus of primary neurons by confocal microscopy we therefore treated cultures with LMB in addition to various secretase inhibitors. Similar to what we observed using rat neurons (Konietzko et al., 2008), the result of LMB treatment was an increased number of nuclear spots staining for AICD (Fig. 8B,D).

Because APP staining in the cytosol labels vesicles with similar dimensions as nuclear spots and because APP is also present in the perinuclear endoplasmic reticulum, it is essential to identify a mid-nuclear plane in the confocal microscope for analysis. We stained neurons with DRAQ5 to label nuclei and in addition with Map2ab to label the neuronal microtubular cytoskeleton. Taking confocal sections with 1-µm steps in the z-axis, we saw that the Map2ab staining more faithfully reveals the mid-nuclear plane (Fig. 8B). Whereas in the middle panel (1 µm below the mid-nuclear plane) the DRAQ5 staining still reveals nuclear dimensions similar to the first panel, the staining for Map2ab shows that the nuclear edges are already overlaid with microtubules. AICD spots identified in this section could therefore represent cytosolic APP. We thus chose to select mid-nuclear confocal planes via the Map2ab staining (Fig. 8B, plane of first panel) before imaging the AICD and nuclear stainings.

To determine the influence of the β-secretase cleavage pathway on the occurrence of endogenous nuclear AICD spots, primary neurons were treated with pharmacological inhibitors to modulate cleavage of either α- or β-secretase. In order to test the efficiency of commercially available inhibitors, neurons were treated for 22 hours at DIV 14 with 20 µM of the α-secretase inhibitor TAPI 1, or with 60 nM BACE1 inhibitor A, or with 1.4 µM BACE1 inhibitor B. In addition, cells were treated concomitantly with 1 µM γ-secretase inhibitor DAPT to accumulate CTFs. As expected, treatment with TAPI 1 resulted in a reduction in α-CTF levels, whereas treatment with either BACE1 inhibitor A or B resulted in a reduction in β-CTFs, when compared to treatment with DAPT alone (Fig. 8C). Neurons were subsequently treated with the different secretase inhibitors together with 20 ng/ml LMB for 22 hours, followed by staining with APP C-terminal and Map2ab antibodies, and analysis by confocal microscopy (Fig. 8D).

Neurons were identified by the Map2ab staining that also guided the identification of the optimal mid-nuclear plane as described above. Single confocal sections from 19-42 neurons were imaged for each condition (control, n=19; LMB, n=35; DAPT + LMB, n=34; TAPI 1 + LMB, n=42; BACE1 inhibitor A + LMB, n=38; BACE1 inhibitor B + LMB, n=22). The nuclei were outlined with the help of the Map2ab staining, and the number of AICD spots quantified by two independent researchers blinded to the experimental conditions (Fig. 8E). After treatment with LMB an increased number of AICD spots was clearly visible in the nucleus, which was not significantly reduced by TAPI 1 co-treatment. By contrast, treatment of neurons with DAPT, which prevents AICD generation, or with either of the BACE1 inhibitors resulted in a significant inhibition of nuclear AICD spot formation (MWU, P<0.001 versus LMB alone). Thus, the inhibition of β-secretase was sufficient to prevent nuclear signaling of endogenous AICD in neurons, whereas α-secretase inhibition had no effect.

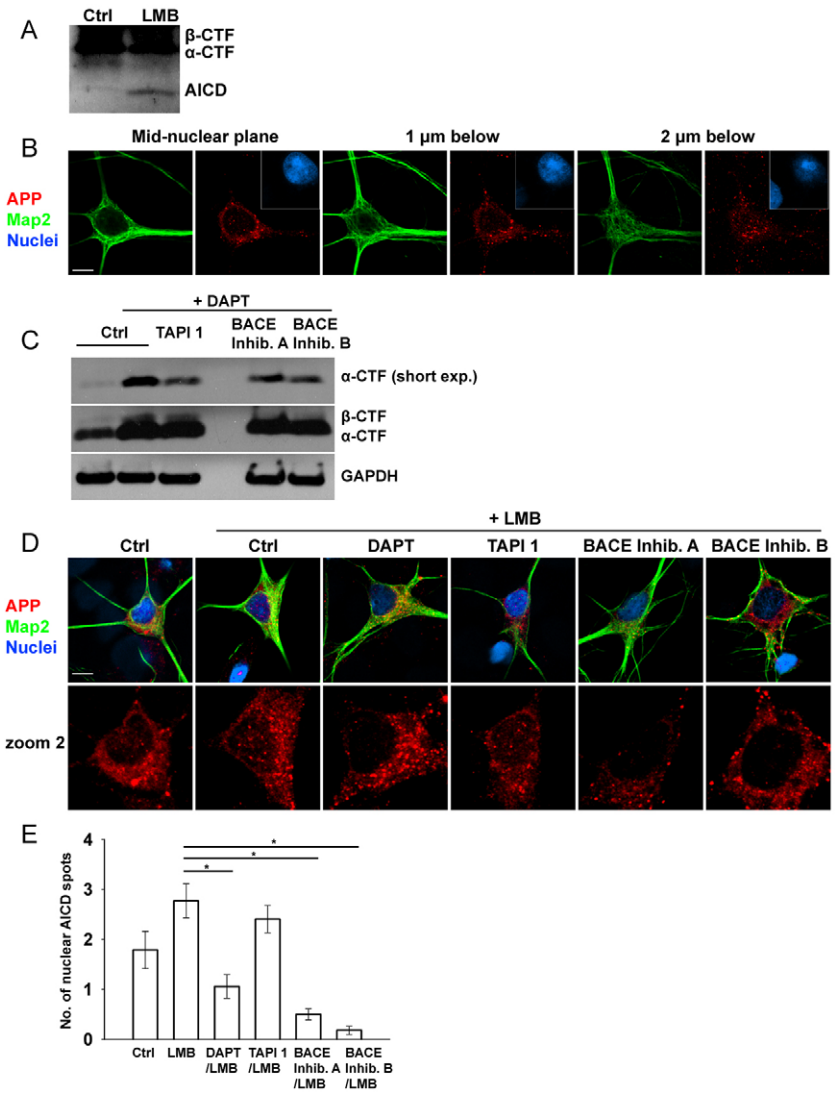

Fig. 8. BACE1 inhibition in primary neurons inhibits endogenous AICD nuclear signaling. (A) Primary neuronal cultures, prepared from postnatal day zero C57/Bl6 mice, were treated at DIV 14 with 20 ng/ml LMB, followed by nuclei isolation and immunoprecipitation. Western blotting with anti-APP C-terminal antibody shows a dramatic increase in the level of AICD detected in the nuclear fraction after LMB treatment. (B) Neurons treated with LMB were fixed in methanol and stained for APP, Map2ab and DNA (DRAQ5). Confocal sections were taken 1 μm apart in the *z*-axis. The first panel shows the mid-nuclear plane, free of Map2ab staining in the DRAQ5-stained nuclei (insert). Moving towards the bottom of the cell the second panel still seems to encompass the nucleus according to the DRAQ5 staining but the Map2ab staining shows that microtubules already overlay with the nuclear staining. The third panel shows the microtubule network lying beneath the nucleus with APP staining in vesicular structures. Scale bar: 7 μm. (C) Primary neuronal cultures at 14 DIV were treated with 20 μM α-secretase inhibitor TAPI 1, 60 nM BACE1 inhibitor A (Calbiochem, #171601) or 1.4 μM BACE1 inhibitor B (Calbiochem, #565749), together with 1 μM γ-secretase inhibitor DAPT to accumulate CTFs. Western blots were stained with APP C-terminal antibodies. Treatment with TAPI 1 leads to a reduction in levels of α-CTFs, whereas treatment with either BACE1 inhibitor A or B leads to a reduction in β-CTFs, when compared to DAPT treatment alone. (D) Neuronal cultures at DIV 14 were treated with LMB for 22 hours and additionally with the different secretase inhibitors as described in C. Cells were stained as in B and single confocal sections were acquired in the mid-nuclear plane as determined by the Map2ab staining. The upper row shows an overlay of all three stainings whereas the lower row is a twofold zoom of the APP staining. Treatment with either LMB alone or in combination with TAPI1 results in a relatively high frequency of AICD nuclear spots. By contrast, treatment of neurons with DAPT or either BACE1 inhibitor A or B reduces the frequency of nuclear AICD spots. Scale bar: 7 μm. (E) Quantification of the number of AICD spots per nucleus reveals a significant reduction in the number of nuclear AICD spots following treatment with either DAPT or BACE1 inhibitors. **P*<0.001 versus LMB alone, MWU. Treatment of cells with TAPI 1 does not significantly alter the number of nuclear AICD spots, when compared to LMB treatment alone. Number of imaged neurons: control, *n*=19; LMB, *n*=35; DAPT+LMB, *n*=34; TAPI 1+LMB, *n*=42; BACE1 inhibitor A+LMB, *n*=38; BACE1 inhibitor B+LMB, *n*=22, error bars represent s.e.m.

Discussion

The physiological outcomes of α- or β-secretase-initiated processing of APP are distinct. We have now shown that this dichotomy holds up for AICD nuclear signaling. The β-secretase-mediated cleavage of APP in endosomal compartments is mainly responsible for generating AICD species that are capable of translocating to the nucleus, and active transport of endosomes to the perinuclear region is a prerequisite for nuclear signaling.

RIP-mediated generation of cytosolic fragments of type I transmembrane proteins is emerging as a widely used pathway for directly transmitting a signal from the plasma membrane to the nucleus (Fortini, 2002). It has been demonstrated that AICD possesses transactivation activity in luciferase assays (Cao and Sudhof, 2001), controls the expression of endogenous target genes (Alves da Costa et al., 2006; Baek et al., 2002; Belyaev et al., 2009; Liu et al., 2007; Muller et al., 2006; Pardossi-Piquard et al., 2005; Schrenk-Siemens et al., 2008; von Rotz et al., 2004; Zhang et al., 2007) and, together with Fe65 and Tip60, localizes to spherical nuclear complexes that are thought to represent sites of transcription (Konietzko et al., 2008; von Rotz et al., 2004). AICD can be generated from APP by two different proteolytic processing pathways and we have analyzed their differential nuclear signaling capacity. Non-amyloidogenic α-secretase processing occurs at the plasma membrane, whereas β-secretase cleavage takes place in endosomal compartments. AICD is rapidly degraded in the cytoplasm (Cupers et al., 2001) and we hypothesized that the subcellular location of AICD generation could therefore influence its capacity for nuclear signaling (Miaczynska et al., 2004).

Inhibiting endocytosis with dominant-negative dynamin reduced nuclear signaling by AICD, as determined by the reduced number of cells forming nuclear AFT complexes. This means that AICD generated directly at the plasma membrane by sequential α- and γ-cleavages has a lower likelihood of translocating to the nucleus. Endocytosis of APP from the plasma membrane has been reported to lead to Aβ generation, and β-secretase processing has been shown to occur in endosomes (Carey et al., 2005; Grbovic et al., 2003; Rajendran et al., 2006). We confirmed these findings by showing that blocking endocytosis prevents the generation of sAPPβ in endosomal vesicles and strongly reduces the production of β-cleaved C-terminal fragments of APP.

To directly analyze the impact of β-cleavage on AICD-mediated nuclear signaling, we inhibited BACE1 using two independent pharmacological inhibitors that clearly suppressed the β-cleavage of APP. Additionally, the inhibitors resulted in a dose-dependent decrease in AICD nuclear signaling. The strong reduction in nuclear AICD translocation is astonishing in light of the fact that less than 10% of APP is processed along the amyloidogenic pathway. We therefore performed experiments aimed at increasing the amyloidogenic processing of APP. The familial Alzheimer's disease Swedish double mutation in APP has been shown to possess a higher affinity for BACE1 and result in a greater production of β-CTFs and Aβ peptides (Citron et al., 1994; Haass et al., 1995). It has been previously suggested that β-cleavage of wild-type and Swedish APP might localize to different subcellular compartments, with wild-type cleavage occurring in the endosomal system and SwAPP being cleaved in post-Golgi secretory vesicles (Haass et al., 1995). By contrast, we have shown both APP and SwAPP β-cleavage to be strongly reduced by inhibiting endocytosis. By staining with antibodies specific for sAPPβ derived from SwAPP, we could detect a clear inhibition of Swedish sAPPβ formation in cells treated with dominant-negative dynamin. Our results further support the current evidence that SwAPP β-cleavage also occurs within the endosomal system (Rajendran et al., 2006; Rajendran et al., 2008; Zou et al., 2007) and that interaction between BACE1 and SwAPP does not take place in the secretory pathway (Goldsbury et al., 2006). Compared to wild-type APP, the Swedish mutation resulted in a significant increase in AICD nuclear signaling. We therefore propose that this effect is caused by an increased affinity of SwAPP for BACE1, which results in a higher proportion of APP cleavage within endosomal vesicles rather than by α-secretase cleavage at the plasma membrane. Therefore, AICD-mediated nuclear signaling can be both positively and negatively regulated by the manipulation of BACE1 cleavage.

Analysis of AFT complex formation in fibroblasts derived from mice deficient for BACE1 (Dominguez et al., 2005) showed nuclear AICD signaling to be practically abolished in these cells. By contrast, cells derived from ADAM10 knockout mice were still able to form AFT complexes in the nucleus. Similar results were obtained when analyzing endogenous AICD signaling in primary neurons. Inhibition of nuclear export by LMB increased AICD in nuclear spots and this could be blocked by two different β-secretase inhibitors, but not by an inhibitor of α-secretase. Therefore, despite representing the minor cleavage pathway of APP, only amyloidogenic processing generates AICD capable of translocating to the nucleus.

If AICD generated at the plasma membrane following α-γ-cleavage is degraded before it reaches the nucleus, then endocytosis of APP should involve translocation to the nuclear vicinity before γ-cleavage releases AICD. Antibodies bound to cell-surface APP were endocytosed together with APP and could be detected in perinuclear compartments 10 minutes after initiating endocytosis. By 30 minutes, the entire surface-bound antibody accumulated close to the nucleus. This rapid subcellular redistribution is probably mediated by active retrograde transport of signaling endosomes, which is more efficient than diffusion, even over relatively short distances (Howe and Mobley, 2004). Active retrograde transport of endocytic vesicles along microtubules is mediated by the dynein motor and the associated dynactin complex (Schroer, 2004). Overexpression of p50 dynamitin or the $p150^{glued}$ CC1 domain, both components of the dynactin complex, disrupts retrograde transport (Burkhardt et al., 1997; King et al., 2003) and we have shown that this also leads to the disruption of nuclear AFT complex formation. Nuclear signaling by AICD therefore depends upon dynein-mediated retrograde transport and is reminiscent of neurotrophin signaling in this respect. NGF- and BDNF-induced rapid nuclear signaling by trkA and trkB receptors has been shown to rely on dynein-based retrograde transport of signaling endosomes (Ehlers et al., 1995; Watson et al., 1999) that can similarly be disrupted by p50 dynamitin (Bhattacharyya et al., 2002). Recently, nuclear translocation and subsequent gene regulation by the transcription factor NF-κB has likewise been shown to be dependent on active retrograde transport (Shrum et al., 2009).

Whereas retrograde transport targets endosomal vesicles to perinuclear regions, anterograde transport along microtubules delivers them to the cell periphery. The overexpression of KIF16B, a member of the kinesin 3 family of motor proteins responsible for anterograde transport of endosomes (Hoepfner et al., 2005), was shown to diminish AFT complex formation. By reducing the number of early endosomes in the perinuclear region, either by disrupting the dynactin complex or by overexpressing kinesin motor proteins, the likelihood of AICD being delivered to the vicinity of the nucleus is diminished and its production at the plasma membrane, following α-secretase cleavage, increases. The re-distribution of early endosomes to the cell periphery might also lead to a reduced residence time of APP and BACE1 together in early endosomes, due to increased recycling to the plasma membrane, which could explain the reduction in β-cleavage of APP following overexpression of KIF16B. Thus, microtubule-based transport is essential for AICD signaling and this might be disrupted in AD, where axonal swellings with accumulated motor proteins have been described early in the disease process (Stokin et al., 2005).

Cleavage of APP by α- and β-secretase-mediated processing has different physiological outcomes and we have determined that the β-pathway-mediated nuclear signaling is dependent upon fast retrograde transport. In analogy, nerve growth factor (NGF)-trkA interaction in the periphery promotes axonal outgrowth, but only NGF-trkA complexes that are internalized and retrogradely transported in signaling endosomes support neuronal survival (Kuruvilla et al., 2004; Ye et al., 2003). The NGF signal increases the retrograde transport of trkA-containing endosomes that also transport activated ERK1 and ERK2 (Delcroix et al., 2003). Neuronal activity has been shown to increase β-cleavage of APP (Cirrito et al., 2005; Kamenetz et al., 2003) but the molecular mechanisms allowing BACE1 to sense neuronal activity are unknown. APP has been demonstrated to interact with APP on adjacent cells (Soba et al., 2005), but whether this interaction has ligand functions as shown for Notch-Delta (Lubman et al., 2004) and Notch-Serrate (Klueg and Muskavitch, 1999) interaction is not known. Interestingly, the trans-endocytosis of ligand-bound Notch extracellular domain (ECD) has been found to be a prerequisite for efficient processing and dissociation of Notch 1 intracellular domain (NICD) and its subsequent nuclear localization (Klueg and Muskavitch, 1999; Parks et al., 2000). It is therefore possible that the release of AICD from APP is also controlled by ligand binding.

One such ligand, which has been described to bind APP and trigger γ-secretase-dependent AICD release, is the GPI-linked recognition molecule TAG1 (Ma et al., 2008). The influence of TAG1 on APP cleavage is analogous to the interaction between GPI-linked Ephrin A and EphA receptors at the cell surface, which has been shown to promote the cleavage of Ephrin A by ADAM10, enabling contact-dependent axon repulsion during neural development (Hattori et al., 2000). Regulation of EphB-EphrinB interaction has alternatively been shown to be dependent on endocytosis of the receptor-ligand complex

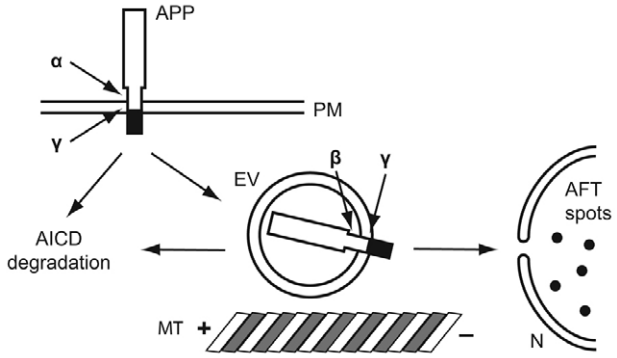

Fig. 9. Schematic representation of nuclear signaling by AICD. APP is synthesized in the ER, transported along the secretory pathway and targeted to the plasma membrane (PM), where sequential cleavages by α- and γ-secretase generate AICD, which is rapidly degraded. Alternatively, APP is taken up into endocytic vesicles (EV), which are anterogradely and retrogradely transported along microtubules (MT). Sequential cleavage of APP by β- and γ-secretases in endosomes generates AICD, which, in the case of preceding retrograde transport, occurs in close vicinity to the nucleus (N). The APP-binding protein Fe65 transports AICD to the nucleus where, together with Tip60, they form nuclear AFT complexes, which are involved in the transcription of AICD-regulated genes.

from the cell surface (Marston et al., 2003; Zimmer et al., 2003). It is therefore plausible that the interaction between TAG1 and APP promotes its endocytosis, which, according to our data, would in turn lead to elevated β-cleavage and enhanced AICD nuclear signaling.

Further support for the connection between AICD signaling and the β-cleavage pathway comes from two recent publications. Ma and colleagues have determined that enhanced synaptic plasticity and learning and memory in APP-overexpressing mice is abolished by the deletion of BACE1 (Ma et al., 2007). Moreover, the authors identified AICD as the only APP-derived fragment that correlated with the changes in synaptic plasticity. Secondly, using Gal4-promoter luciferase assays in primary neurons, Hoey and colleagues have shown inhibition of APP-Gal4-mediated luciferase activity after treatment with a β-secretase inhibitor, but not after treatment with TAPI 1 (Hoey et al., 2009). As we have discussed previously, the transcription of luciferase from transiently transfected plasmids that lack a nuclear localization sequence occurs in the cytosol (Konietzko et al., 2008). Plasmids can enter the nucleus only after nuclear membrane breakdown during mitosis, which does not occur in differentiated neurons. Nevertheless, the plasmids are retrogradely transported to the vicinity of the nucleus and thus are only accessible for AICD-Gal4 that reaches the perinuclear space. The data of Hoey and colleagues therefore provide clear support for our findings that the endocytic β-secretase cleavage pathway and retrograde transport are prerequisites for AICD nuclear signaling.

Shuttling of AICD into the nucleus is promoted by APP-bound protein complexes containing Fe65 (Kimberly et al., 2001; von Rotz et al., 2004) and 14-3-3 γ (Sumioka et al., 2005) and inhibited by the neuronal adaptor proteins X11/MINT, which compete with Fe65 for binding to APP (Lau et al., 2000; von Rotz et al., 2004). In addition, the control of nuclear export can influence the level of nuclear AICD signaling, because inhibition of nuclear export leads to the accumulation of AICD in nuclear spots when Fe65 is coexpressed (Konietzko et al., 2008; von Rotz et al., 2004). Nuclear signaling by AICD can therefore be modulated by multiple signals acting at different stages of the APP life cycle. It has been recently demonstrated that stimulation of the β2-adrenergic or δ-opioid receptors leads to agonist-induced endocytosis that traffics γ-secretase to late endosomes and elevates Aβ and AICD levels (Ni et al., 2007). In the light of our data showing that nuclear AICD translocation relies upon endocytic β-γ processing, this signaling can therefore probably also be regulated by neurotransmitters.

In summary, our data suggest that endocytic APP processing along the amyloidogenic pathway generates AICD capable of regulating transcription, whereas AICD generated by α-cleavage at the plasma membrane is likely to be degraded before reaching the nucleus (Fig. 9). Most APP is processed by α-secretase, even in neurons that express the highest levels of BACE1. Thus, regulating the rate of β-cleavage of APP will have profound effects on nuclear signaling by AICD. Increased β-secretase processing of APP leads to AD, which is attributed to the generation of Aβ peptides. Because nuclear AFT complexes have been shown to mediate transcription, and in particular to regulate genes linked to AD pathology, the regulation of AICD-mediated nuclear signaling could play a role in the disease process. Further investigation into the biological function of AICD nuclear signaling will be necessary to predict the outcome of BACE1 inhibition as a therapy to reduce Aβ production in AD.

Materials and Methods

Cell culture

Human embryonic kidney cells (HEK293), mouse embryonic fibroblasts and HeLa cells were cultured as previously described (Rajendran et al., 2006; von Rotz et al., 2004). For transfection, Lipofectamine 2000 was used according to the manufacturer's protocol. Leptomycin B DAPT, TAPI 1, BACE1 inhibitors A and B were from Calbiochem. Sterol-linked BACE1 inhibitor (Rajendran et al., 2008) was used at 1 μM.

Primary cell culture

Primary neuronal cultures were prepared from 1-day-old C57Bl/6 mouse pups. Cortices and hippocampi were dissected, transferred into EBSS (Invitrogen) containing 20U Papain (BioConcept) for 20 minutes at 37°C and triturated in Dulbecco's modified Eagle's medium (DMEM; Invitrogen) containing 10% horse serum. Cells were plated at a density of 5000 cells/mm^2 onto coverslips coated with poly-D-lysine (0.01%) and laminin (1.5 μg/cm^2). After 3 hours, the medium was changed to Neurobasal A (Invitrogen) containing B27 (Invitrogen), 200 mM L-glutamine and 100 mM sodium pyruvate. Cells were cultured for 14 days at 37°C, 5% CO_2.

Expression constructs

Wild-type dynamin-HA, dominant-negative dynamin-K44A-HA and dynamin-K44A-GFP (Herskovits et al., 1993); APP-Citrine, HA-Fe65, Myc-Fe65 and CFP-Tip60 (von Rotz et al., 2004); RFP-p150^{Glued} (Quintyne et al., 1999); p50-dynamitin-GFP (Burkhardt et al., 1997); wild-type KIF16B, dominant-negative KIF16B-ΔN (Hoepfner et al., 2005). Site-directed mutagenesis, yielded SwAPP constructs (Citron et al., 1995). CMV-promoter-driven expression vectors containing C-terminal in frame extensions with the fluorescent protein Citrine or a triple HA tag were used for cloning. HEK293 cell lines expressing APP-3HA and APP-Citrine were developed by manual cell sorting.

Live antibody incubation

HEK293 cells, transfected with HA-tagged APP, were incubated with 6E10 (1:100, Signet) antibodies at 4°C for 30 minutes. Cells were either fixed immediately or incubated further for 10 or 30 minutes at 37°C to allow endocytosis of APP-antibody complexes.

Transferrin uptake experiments

Hela-SwAPP cells were transfected with control GFP or dynamin-K44A-GFP. After 6 hours, the cells were incubated with iron-loaded human rhodamine-transferrin (10 μg/ml) for 10 minutes at 37°C.

Immunocytochemistry

Immunocytochemistry was performed as previously described (Rajendran et al., 2006; von Rotz et al., 2004). Mouse anti-Myc (Roche) rat anti-HA (Roche) and rabbit anti-APP C terminus (Vingtdeux et al., 2007; Vingtdeux et al., 2005) antibodies were applied at 1:100 dilution, mouse anti Map2ab (Sigma) at 1:200, and anti-sAPPβ as described (Rajendran et al., 2006). Cy3 or Cy5-conjugated secondary antibodies (Jackson Laboratories) were applied at 1:250 dilutions. Cells were embedded in Mowiol. DRAQ5 (Biostatus) or DAPI (Sigma) were used to stain nuclei.

Nuclei isolation

Cells were homogenized on ice using 10 strokes in a dounce homogenizer in buffer containing 20 mM HEPES (pH 7.4), 20 mM KCl, 2 mM $MgCl_2$, 2 mM DTT, 1.5 mM PMSF, 5 mM Phenantroline, 3 mM EGTA, 250 μg/ml insulin, 0.5 mM spermidine, 0.15 mM spermine, and Protease Inhibitor Cocktail (Roche). After addition of 0.5% NP-40 and 0.25 M sucrose, homogenization was repeated for a further 10 strokes before centrifugation for 10 minutes at 800 ***g***.

Immunoprecipitation

Immunoprecipitations were carried out using anti-APP C-terminus and anti-Tip60 (Calbiochem) antibodies using standard protocols.

Western blotting

For western blotting, anti-HA antibody (1:1000; Roche), APP-C-terminal antibody (1:2000; Sigma), 6E10 (1:500; Signet), Dynamin-1 antibody (1:200; Santa Cruz Biotechnology) and anti-GFP (1:1000; Invitrogen) were used. Bands were visualized by ECL (Pierce).

Fluorescence microscopy

Counting of cells containing nuclear AFT complexes was performed using a Leica DM IRE2 inverted microscope by two independent researchers, blinded to the transfection conditions. The total number of cells with AFT complexes was determined and normalized for transfection efficiency by comparing the levels of Citrine, CFP or Cy3 fluorescence. With 5×10^4 cells plated per well, we identified between 25 and 600 cells with nuclear AFT complexes, depending on cell type and transfected plasmids. Relative number of cells with AFT complexes (Fig. 3A) was calculated by dividing the total number of cells with AFT complexes in a well by the total number of cells with AFT complexes in the experiment.

Confocal microscopy

Images were acquired on a Leica TCS/SP2 confocal microscope (Leica, Wetzlar, Germany) as described (von Rotz et al., 2004)

We are grateful to Michelle Meier for excellent technical assistance. We gratefully acknowledge Sebastian Hoepfner and Marino Zerial (MPI for Molecular Cell Biology and Genetics, Dresden, Germany) for providing us with the KIF16B constructs. We would like to thank Urs Greber (University of Zurich, Zurich, Switzerland) for supplying us with constructs expressing p50 dynamitin (originally from Richard Vallee) and $p150^{Glued}$ (originally from Trina Schroer). We also want to acknowledge Bart de Strooper (Katholieke Universiteit, Leuven, Belgium) for providing BACE1 and ADAM10 knockout fibroblasts. This work was supported by the Transregio SFB (6027) on Structure and Function of Membrane Proteins, the SNF NCCR on Neural Plasticity and Repair and the EU grant LSHM-CT-2003-503330 (APOPIS). L.R. is supported by grants from the Alzheimer Forschung Initiative e.V and the SNF NCCR on Neural Plasticity and Repair.

References

Abbenante, G., Kovacs, D. M., Leung, D. L., Craik, D. J., Tanzi, R. E. and Fairlie, D. P. (2000). Inhibitors of beta-amyloid formation based on the beta-secretase cleavage site. *Biochem. Biophys. Res. Commun.* **268**, 133-135.

Alves da Costa, C., Sunyach, C., Pardossi-Piquard, R., Sevalle, J., Vincent, B., Boyer, N., Kawarai, T., Girardot, N., St George-Hyslop, P. and Checler, F. (2006). Presenilin-dependent gamma-secretase-mediated control of p53-associated cell death in Alzheimer's disease. *J. Neurosci.* **26**, 6377-6385.

Annaert, W. G., Levesque, L., Craessaerts, K., Dierinck, I., Snellings, G., Westaway, D., George-Hyslop, P. S., Cordell, B., Fraser, P. and De Strooper, B. (1999). Presenilin 1 controls gamma-secretase processing of amyloid precursor protein in pre-golgi compartments of hippocampal neurons. *J. Cell Biol.* **147**, 277-294.

Baek, S. H., Ohgi, K. A., Rose, D. W., Koo, E. H., Glass, C. K. and Rosenfeld, M. G. (2002). Exchange of N-CoR corepressor and Tip60 coactivator complexes links gene expression by NF-kappaB and beta-amyloid precursor protein. *Cell* **110**, 55-67.

Belyaev, N. D., Nalivaeva, N. N., Makova, N. Z. and Turner, A. J. (2009). Neprilysin gene expression requires binding of the amyloid precursor protein intracellular domain to its promoter: implications for Alzheimer disease. *EMBO Rep.* **10**, 94-100.

Bhattacharyya, A., Watson, F. L., Pomeroy, S. L., Zhang, Y. Z., Stiles, C. D. and Segal, R. A. (2002). High-resolution imaging demonstrates dynein-based vesicular transport of activated Trk receptors. *J. Neurobiol.* **51**, 302-312.

Burkhardt, J. K., Echeverri, C. J., Nilsson, T. and Vallee, R. B. (1997). Overexpression of the dynamitin (p50) subunit of the dynactin complex disrupts dynein-dependent maintenance of membrane organelle distribution. *J. Cell Biol.* **139**, 469-484.

Cao, X. and Sudhof, T. C. (2001). A transcriptionally [correction of transcriptively] active complex of APP with Fe65 and histone acetyltransferase Tip60. *Science* **293**, 115-120.

Carey, R. M., Balcz, B. A., Lopez-Coviella, I. and Slack, B. E. (2005). Inhibition of dynamin-dependent endocytosis increases shedding of the amyloid precursor protein ectodomain and reduces generation of amyloid beta protein. *BMC Cell Biol.* **6**, 30.

Chyung, J. H., Raper, D. M. and Selkoe, D. J. (2005). Gamma-secretase exists on the plasma membrane as an intact complex that accepts substrates and effects intramembrane cleavage. *J. Biol. Chem.* **280**, 4383-4392.

Cirrito, J. R., Yamada, K. A., Finn, M. B., Sloviter, R. S., Bales, K. R., May, P. C., Schoepp, D. D., Paul, S. M., Mennerick, S. and Holtzman, D. M. (2005). Synaptic activity regulates interstitial fluid amyloid-beta levels in vivo. *Neuron* **48**, 913-922.

Citron, M., Vigo-Pelfrey, C., Teplow, D. B., Miller, C., Schenk, D., Johnston, J., Winblad, B., Venizelos, N., Lannfelt, L. and Selkoe, D. J. (1994). Excessive production of amyloid beta-protein by peripheral cells of symptomatic and presymptomatic patients carrying the Swedish familial Alzheimer disease mutation. *Proc. Natl. Acad. Sci. USA* **91**, 11993-11997.

Citron, M., Teplow, D. B. and Selkoe, D. J. (1995). Generation of amyloid beta protein from its precursor is sequence specific. *Neuron* **14**, 661-670.

Cupers, P., Orlans, I., Craessaerts, K., Annaert, W. and De Strooper, B. (2001). The amyloid precursor protein (APP)-cytoplasmic fragment generated by gamma-secretase is rapidly degraded but distributes partially in a nuclear fraction of neurones in culture. *J. Neurochem.* **78**, 1168-1178.

Delcroix, J. D., Valletta, J. S., Wu, C., Hunt, S. J., Kowal, A. S. and Mobley, W. C. (2003). NGF signaling in sensory neurons: evidence that early endosomes carry NGF retrograde signals. *Neuron* **39**, 69-84.

Dominguez, D., Tournoy, J., Hartmann, D., Huth, T., Cryns, K., Deforce, S., Serneels, L., Camacho, I. E., Marjaux, E., Craessaerts, K. et al. (2005). Phenotypic and biochemical analyses of BACE1- and BACE2-deficient mice. *J. Biol. Chem.* **280**, 30797-30806.

Edbauer, D., Willem, M., Lammich, S., Steiner, H. and Haass, C. (2002). Insulin-degrading enzyme rapidly removes the beta-amyloid precursor protein intracellular domain (AICD). *J. Biol. Chem.* **277**, 13389-13393.

Ehehalt, R., Keller, P., Haass, C., Thiele, C. and Simons, K. (2003). Amyloidogenic processing of the Alzheimer beta-amyloid precursor protein depends on lipid rafts. *J. Cell Biol.* **160**, 113-123.

Ehlers, M. D., Kaplan, D. R., Price, D. L. and Koliatsos, V. E. (1995). NGF-stimulated retrograde transport of trkA in the mammalian nervous system. *J. Cell Biol.* **130**, 149-156.

Ferreira, A., Caceres, A. and Kosik, K. S. (1993). Intraneuronal compartments of the amyloid precursor protein. *J. Neurosci.* **13**, 3112-3123.

Fortini, M. E. (2002). Gamma-secretase-mediated proteolysis in cell-surface-receptor signalling. *Nat. Rev. Mol. Cell Biol.* **3**, 673-684.

Fukumori, A., Okochi, M., Tagami, S., Jiang, J., Itoh, N., Nakayama, T., Yanagida, K., Ishizuka-Katsura, Y., Morihara, T., Kamino, K. et al. (2006). Presenilin-dependent gamma-secretase on plasma membrane and endosomes is functionally distinct. *Biochemistry* **45**, 4907-4914.

Goldsbury, C., Mocanu, M. M., Thies, E., Kaether, C., Haass, C., Keller, P., Biernat, J., Mandelkow, E. and Mandelkow, E. M. (2006). Inhibition of APP trafficking by tau protein does not increase the generation of amyloid-beta peptides. *Traffic* **7**, 873-888.

Grbovic, O. M., Mathews, P. M., Jiang, Y., Schmidt, S. D., Dinakar, R., Summers-Terio, N. B., Ceresa, B. P., Nixon, R. A. and Cataldo, A. M. (2003). Rab5-stimulated up-regulation of the endocytic pathway increases intracellular beta-cleaved amyloid precursor protein carboxyl-terminal fragment levels and Abeta production. *J. Biol. Chem.* **278**, 31261-31268.

Haass, C., Lemere, C. A., Capell, A., Citron, M., Seubert, P., Schenk, D., Lannfelt, L. and Selkoe, D. J. (1995). The Swedish mutation causes early-onset Alzheimer's disease by beta-secretase cleavage within the secretory pathway. *Nat. Med.* **1**, 1291-1296.

Hardy, J. and Selkoe, D. J. (2002). The amyloid hypothesis of Alzheimer's disease: progress and problems on the road to therapeutics. *Science* **297**, 353-356.

Hardy, J. A. and Higgins, G. A. (1992). Alzheimer's disease: the amyloid cascade hypothesis. *Science* **256**, 184-185.

Hattori, M., Osterfield, M. and Flanagan, J. G. (2000). Regulated cleavage of a contact-mediated axon repellent. *Science* **289**, 1360-1365.

Herskovits, J. S., Burgess, C. C., Obar, R. A. and Vallee, R. B. (1993). Effects of mutant rat dynamin on endocytosis. *J. Cell Biol.* **122**, 565-578.

Hoepfner, S., Severin, F., Cabezas, A., Habermann, B., Runge, A., Gillooly, D., Stenmark, H. and Zerial, M. (2005). Modulation of receptor recycling and degradation by the endosomal kinesin KIF16B. *Cell* **121**, 437-450.

Hoey, S. E., Williams, R. J. and Perkinton, M. S. (2009). Synaptic NMDA receptor activation stimulates alpha-secretase amyloid precursor protein processing and inhibits amyloid-beta production. *J. Neurosci.* **29**, 4442-4460.

Howe, C. L. and Mobley, W. C. (2004). Signaling endosome hypothesis: a cellular mechanism for long distance communication. *J. Neurobiol.* **58**, 207-216.

Huse, J. T., Pijak, D. S., Leslie, G. J., Lee, V. M. and Doms, R. W. (2000). Maturation and endosomal targeting of beta-site amyloid precursor protein-cleaving enzyme: the Alzheimer's disease beta-secretase. *J. Biol. Chem.* **275**, 33729-33737.

Kakuda, N., Funamoto, S., Yagishita, S., Takami, M., Osawa, S., Dohmae, N. and Ihara, Y. (2006). Equimolar production of amyloid beta-protein and amyloid precursor protein intracellular domain from beta-carboxyl-terminal fragment by gamma-secretase. *J. Biol. Chem.* **281**, 14776-14786.

Kamenetz, F., Tomita, T., Hsieh, H., Seabrook, G., Borchelt, D., Iwatsubo, T., Sisodia, S. and Malinow, R. (2003). APP processing and synaptic function. *Neuron* **37**, 925-937.

Kimberly, W. T., Zheng, J. B., Guenette, S. Y. and Selkoe, D. J. (2001). The intracellular domain of the beta-amyloid precursor protein is stabilized by Fe65 and translocates to the nucleus in a notch-like manner. *J. Biol. Chem.* **276**, 40288-40292.

King, S. J., Brown, C. L., Maier, K. C., Quintyne, N. J. and Schroer, T. A. (2003). Analysis of the dynein-dynactin interaction in vitro and in vivo. *Mol. Biol. Cell* **14**, 5089-5097.

Kinoshita, A., Fukumoto, H., Shah, T., Whelan, C. M., Irizarry, M. C. and Hyman, B. T. (2003). Demonstration by FRET of BACE interaction with the amyloid precursor protein at the cell surface and in early endosomes. *J. Cell Sci.* **116**, 3339-3346.

Klueg, K. M. and Muskavitch, M. A. (1999). Ligand-receptor interactions and trans-endocytosis of Delta, Serrate and Notch: members of the Notch signalling pathway in Drosophila. *J. Cell Sci.* **112**, 3289-3297.

Konietzko, U., Goodger, Z. V., Meyer, M., Kohli, B. M., Bosset, J., Lahiri, D. K. and Nitsch, R. M. (2008). Co-localization of the amyloid precursor protein and Notch intracellular domains in nuclear transcription factories. *Neurobiol. Aging* [Epub ahead of print] doi:10.1016/j.neurobiolaging.2008.03.001

Koo, E. H. and Squazzo, S. L. (1994). Evidence that production and release of amyloid beta-protein involves the endocytic pathway. *J. Biol. Chem.* **269**, 17386-17389.

Kuruvilla, R., Zweifel, L. S., Glebova, N. O., Lonze, B. E., Valdez, G., Ye, H. and Ginty, D. D. (2004). A neurotrophin signaling cascade coordinates sympathetic neuron development through differential control of TrkA trafficking and retrograde signaling. *Cell* **118**, 243-255.

Lau, K. F., McLoughlin, D. M., Standen, C. L., Irving, N. G. and Miller, C. C. (2000). Fe65 and X11beta co-localize with and compete for binding to the amyloid precursor protein. *NeuroReport* **11**, 3607-3610.

Lin, X., Koelsch, G., Wu, S., Downs, D., Dashti, A. and Tang, J. (2000). Human aspartic protease memapsin 2 cleaves the beta-secretase site of beta-amyloid precursor protein. *Proc. Natl. Acad. Sci. USA* **97**, 1456-1460.

Liu, Q., Zerbinatti, C. V., Zhang, J., Hoe, H. S., Wang, B., Cole, S. L., Herz, J., Muglia, L. and Bu, G. (2007). Amyloid precursor protein regulates brain apolipoprotein E and cholesterol metabolism through lipoprotein receptor LRP1. *Neuron* **56**, 66-78.

Lubman, O. Y., Korolev, S. V. and Kopan, R. (2004). Anchoring notch genetics and biochemistry; structural analysis of the ankyrin domain sheds light on existing data. *Mol. Cell* **13**, 619-626.

Ma, H., Lesne, S., Kotilinek, L., Steidl-Nichols, J. V., Sherman, M., Younkin, L., Younkin, S., Forster, C., Sergeant, N., Delacourte, A. et al. (2007). Involvement of beta-site APP cleaving enzyme 1 (BACE1) in amyloid precursor protein-mediated enhancement of memory and activity-dependent synaptic plasticity. *Proc. Natl. Acad. Sci. USA* **104**, 8167-8172.

Ma, Q. H., Futagawa, T., Yang, W. L., Jiang, X. D., Zeng, L., Takeda, Y., Xu, R. X., Bagnard, D., Schachner, M., Furley, A. J. et al. (2008). A TAG1-APP signalling pathway through Fe65 negatively modulates neurogenesis. *Nat. Cell Biol.* **10**, 283-294.

Marston, D. J., Dickinson, S. and Nobes, C. D. (2003). Rac-dependent trans-endocytosis of ephrinBs regulates Eph-ephrin contact repulsion. *Nat. Cell Biol.* **5**, 879-888.

Mattson, M. P., Cheng, B., Culwell, A. R., Esch, F. S., Lieberburg, I. and Rydel, R. E. (1993). Evidence for excitoprotective and intraneuronal calcium-regulating roles for secreted forms of the beta-amyloid precursor protein. *Neuron* **10**, 243-254.

Miaczynska, M., Christoforidis, S., Giner, A., Shevchenko, A., Uttenweiler-Joseph, S., Habermann, B., Wilm, M., Parton, R. G. and Zerial, M. (2004). APPL proteins link Rab5 to nuclear signal transduction via an endosomal compartment. *Cell* **116**, 445-456.

Muller, T., Concannon, C. G., Ward, M. W., Walsh, C. M., Tirniceriu, A. L., Tribl, F., Kogel, D., Prehn, J. H. and Egensperger, R. (2006). Modulation of gene expression and cytoskeletal dynamics by the APP Intracellular Domain (AICD). *Mol. Biol. Cell* **18**, 201-210.

Neumann, S., Schobel, S., Jager, S., Trautwein, A., Haass, C., Pietrzik, C. U. and Lichtenthaler, S. F. (2006). Amyloid precursor-like protein 1 influences endocytosis and proteolytic processing of the amyloid precursor protein. *J. Biol. Chem.* **281**, 7583-7594.

Ni, Y., Zhao, X., Bao, G., Zou, L., Teng, L., Wang, Z., Song, M., Xiong, J., Bai, Y. and Pei, G. (2007). Activation of beta(2)-adrenergic receptor stimulates gamma-secretase activity and accelerates amyloid plaque formation. *Nat. Med.* **12**, 1390-1396.

Pardossi-Piquard, R., Petit, A., Kawarai, T., Sunyach, C., Alves da Costa, C., Vincent, B., Ring, S., D'Adamio, L., Shen, J., Muller, U. et al. (2005). Presenilin-dependent transcriptional control of the Abeta-degrading enzyme neprilysin by intracellular domains of betaAPP and APLP. *Neuron* **46**, 541-554.

Parks, A. L., Klueg, K. M., Stout, J. R. and Muskavitch, M. A. (2000). Ligand endocytosis drives receptor dissociation and activation in the Notch pathway. *Development* **127**, 1373-1385.

Perez, R. G., Soriano, S., Hayes, J. D., Ostaszewski, B., Xia, W., Selkoe, D. J., Chen, X., Stokin, G. B. and Koo, E. H. (1999). Mutagenesis identifies new signals for beta-amyloid precursor protein endocytosis, turnover, and the generation of secreted fragments, including Abeta42. *J. Biol. Chem.* **274**, 18851-18856.

Quintyne, N. J., Gill, S. R., Eckley, D. M., Crego, C. L., Compton, D. A. and Schroer, T. A. (1999). Dynactin is required for microtubule anchoring at centrosomes. *J. Cell Biol.* **147**, 321-334.

Rajendran, L., Honsho, M., Zahn, T. R., Keller, P., Geiger, K. D., Verkade, P. and Simons, K. (2006). Alzheimer's disease beta-amyloid peptides are released in association with exosomes. *Proc. Natl. Acad. Sci. USA* **103**, 11172-11177.

Rajendran, L., Schneider, A., Schlechtingen, G., Weidlich, S., Ries, J., Braxmeier, T., Schwille, P., Schulz, J. B., Schroeder, C., Simons, M. et al. (2008). Efficient inhibition of the Alzheimer's disease beta-secretase by membrane targeting. *Science* **320**, 520-523.

Schrenk-Siemens, K., Perez-Alcala, S., Richter, J., Lacroix, E., Rahuel, J., Korte, M., Muller, U., Barde, Y. and Bibel, M. (2008). Embryonic Stem cell-derived neurons as a cellular system to study gene function: lack of amyloid precursor proteins APP and APLP2 leads to defective synaptic transmission. *Stem Cells* **26**, 2153-2163.

Schroer, T. A. (2004). Dynactin. *Annu. Rev. Cell Dev. Biol.* **20**, 759-779.

Shrum, C. K., Defrancisco, D. and Meffert, M. K. (2009). Stimulated nuclear translocation of NF-kappaB and shuttling differentially depend on dynein and the dynactin complex. *Proc. Natl. Acad. Sci. USA* **106**, 2647-2652.

Sisodia, S. S. (1992). Beta-amyloid precursor protein cleavage by a membrane-bound protease. *Proc. Natl. Acad. Sci. USA* **89**, 6075-6079.

Soba, P., Eggert, S., Wagner, K., Zentgraf, H., Siehl, K., Kreger, S., Lower, A., Langer, A., Merdes, G., Paro, R. et al. (2005). Homo- and heterodimerization of APP family members promotes intercellular adhesion. *EMBO J.* **24**, 3624-3634.

Stokin, G. B., Lillo, C., Falzone, T. L., Brusch, R. G., Rockenstein, E., Mount, S. L., Raman, R., Davies, P., Masliah, E., Williams, D. S. et al. (2005). Axonopathy and transport deficits early in the pathogenesis of Alzheimer's disease. *Science* **307**, 1282-1288.

Sumioka, A., Nagaishi, S., Yoshida, T., Lin, A., Miura, M. and Suzuki, T. (2005). Role of 14-3-3gamma in FE65-dependent gene transactivation mediated by the amyloid beta-protein precursor cytoplasmic fragment. *J. Biol. Chem.* **280**, 42364-42374.

Tarassishin, L., Yin, Y. I., Bassit, B. and Li, Y. M. (2004). Processing of Notch and amyloid precursor protein by gamma-secretase is spatially distinct. *Proc. Natl. Acad. Sci. USA* **101**, 17050-17055.

Vassar, R., Bennett, B. D., Babu-Khan, S., Kahn, S., Mendiaz, E. A., Denis, P., Teplow, D. B., Ross, S., Amarante, P., Loeloff, R. et al. (1999). Beta-secretase cleavage of Alzheimer's amyloid precursor protein by the transmembrane aspartic protease BACE. *Science* **286**, 735-741.

Vingtdeux, V., Hamdane, M., Gompel, M., Begard, S., Drobecq, H., Ghestem, A., Grosjean, M. E., Kostanjevecki, V., Grognet, P., Vanmechelen, E. et al. (2005). Phosphorylation of amyloid precursor carboxy-terminal fragments enhances their processing by a gamma-secretase-dependent mechanism. *Neurobiol Dis.* **20**, 625-637.

Vingtdeux, V., Hamdane, M., Begard, S., Loyens, A., Delacourte, A., Beauvillain, J. C., Buee, L., Marambaud, P. and Sergeant, N. (2007). Intracellular pH regulates amyloid precursor protein intracellular domain accumulation. *Neurobiol Dis.* **25**, 686-696.

von Rotz, R. C., Kohli, B. M., Bosset, J., Meier, M., Suzuki, T., Nitsch, R. M. and Konietzko, U. (2004). The APP intracellular domain forms nuclear multiprotein complexes and regulates the transcription of its own precursor. *J. Cell Sci.* **117**, 4435-4448.

Walsh, D. M., Klyubin, I., Fadeeva, J. V., Cullen, W. K., Anwyl, R., Wolfe, M. S., Rowan, M. J. and Selkoe, D. J. (2002). Naturally secreted oligomers of amyloid beta protein potently inhibit hippocampal long-term potentiation in vivo. *Nature* **416**, 535-539.

Watson, F. L., Heerssen, H. M., Moheban, D. B., Lin, M. Z., Sauvageot, C. M., Bhattacharyya, A., Pomeroy, S. L. and Segal, R. A. (1999). Rapid nuclear responses to target-derived neurotrophins require retrograde transport of ligand-receptor complex. *J. Neurosci.* **19**, 7889-7900.

Ye, H., Kuruvilla, R., Zweifel, L. S. and Ginty, D. D. (2003). Evidence in support of signaling endosome-based retrograde survival of sympathetic neurons. *Neuron* **39**, 57-68.

Zhang, Y. W., Wang, R., Liu, Q., Zhang, H., Liao, F. F. and Xu, H. (2007). Presenilin/{gamma}-secretase-dependent processing of beta-amyloid precursor protein regulates EGF receptor expression. *Proc. Natl. Acad. Sci. USA* **104**, 10613-10618.

Zimmer, M., Palmer, A., Kohler, J. and Klein, R. (2003). EphB-ephrinB bi-directional endocytosis terminates adhesion allowing contact mediated repulsion. *Nat. Cell Biol.* **5**, 869-878.

Zou, L., Wang, Z., Shen, L., Bao, G. B., Wang, T., Kang, J. H. and Pei, G. (2007). Receptor tyrosine kinases positively regulate BACE activity and Amyloid-beta production through enhancing BACE internalization. *Cell Res.* **17**, 389-401.